Populating the landscape in an inhomogeneous universe

Pu-Xin Lin[1,2,*] and Yun-Song Piao[1,2,3,4,†]

[1]*School of Physics, University of Chinese Academy of Sciences, Beijing 100049, China*
[2]*Institute of Theoretical Physics, Chinese Academy of Sciences, P.O. Box 2735, Beijing 100190, China*
[3]*School of Fundamental Physics and Mathematical Sciences, Hangzhou Institute for Advanced Study, UCAS, Hangzhou 310024, China*
[4]*International Center for Theoretical Physics Asia-Pacific, P.O. Box 2735, Beijing 100190, China*

(Received 22 November 2021; accepted 2 March 2022; published 28 March 2022)

The primordial universe might be highly inhomogeneous. We perform the $(3+1)$D numerical relativity simulation for the evolution of scalar field in an initial inhomogeneous expanding universe, and investigate how it populates the landscape with both de Sitter (dS) and anti–de Sitter (AdS) vacua. The simulation results show that eventually either the field in different region separates into different vacua, so that the expanding dS or AdS bubbles (the bubble wall is expanding but the spacetime inside AdS bubbles is contracting) come into being with clear boundaries, or overall region is dS expanding with a few smaller AdS bubbles (which collapsed into black holes) or inhomogeneously collapsing.

DOI: 10.1103/PhysRevD.105.063534

I. INTRODUCTION

It has been widely thought that the inflation [1–6], which may be well approximated by a de Sitter (dS) spacetime, should happen at the early epoch of our universe. The current accelerated expansion of our universe also suggests that it has a dS-like dark energy referred to as the cosmological constant. However, a stable dS state seems not favorable in the string landscape [7,8], which, if it exists, might be extremely rare, see Refs. [9,10] for the swampland conjecture. In contrast, it is easy to construct anti-dS (AdS) vacua, [7,11], see, e.g., [12–18] for the implications of AdS vacua on the early universe.

In such a landscape (AdS and dS vacua coexist), see Fig. 1, whether it is possible for our universe to evolve to the corresponding dS vacua and whether it is possible for it to stay in a dS state consistent with the current observations is not obvious. Thus how to populate the landscape, especially how our universe started from a dS-like inflation when AdS vacua exist, has still been a concerning issue. It has been showed in Refs. [19,20] that, in an effective potential with multiple vacua, the nucleation of bubbles with different vacua can spontaneously occur, see also, e.g., [21–26]. Recent Refs. [27–29] have also reported the possibility that a large velocity fluctuation of the scalar field pushes a region of field over the potential barrier.

However, it is usually speculated that the primordial universe is highly inhomogeneous, i.e., the scalar field or spacetime metric has large inhomogeneities before a region of space arrived at a certain vacuum. The large inhomogeneities might also be present in multistream inflation [30,31], in which the inflaton field rolled along a multiple-branch path, so that the homogeneities might hardly be preserved after bifurcations, see also recent [32]. Recently, in the studies concerning large inhomogeneities, numerical relativity (NR), see Refs. [33–35] for recent reviews, has become a powerful and indispensable tool [36–40], see also its application to the beginning of inflation [41–45], cosmological bubble collisions [46–49], cosmological solitons [50] and primordial black holes [51].

It is interesting and significant to perform the $(3+1)$D NR simulation in an initial inhomogeneous universe to investigate how the scalar field populates the landscape. We will work with a highly inhomogeneous universe that is initially expanding and a scalar field (its effective potential has both dS and AdS vacua), and numerically evolve it with modified NR package GRCHOMBO[1] [52]. This paper is outlined as follows. In Sec. II, we present the model and initial conditions. In Sec. III, we present the simulation results and discuss the relevant implications. We conclude in Sec. IV. We will set $c = 8\pi G = 1$. Throughout the paper, we will set the reduced Planck mass $\tilde{M}_{\rm Pl} = 1$.

II. THE MODEL AND INITIAL CONDITIONS

In an effective theory, the string landscape might correspond to a complex and rugged potential. However, for

*linpiaoxin17@mails.ucas.ac.cn
†yspiao@ucas.ac.cn

[1]http://www.grchombo.org; https://github.com/GRChombo.

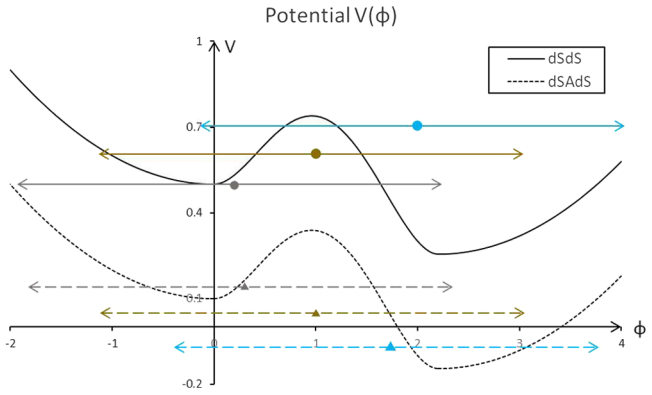

FIG. 1. The upper panel is the dSdS potential (both minima are dS-like), the lower panel is the dSAdS potential (one minimum is dS-like, the other is AdS-like). Lengths of the arrow lines represent the initial amplitude of ϕ. The brown, gray, blue colored lines and dotted lines correspond to different sets in our simulations, i.e., the first, second and third set, respectively.

simplicity, we set the potential $\sim\phi^2$ around its minima,[2] which are separated by a fourth-order polynomial barrier,

$$V(\phi)=\begin{cases}\frac{1}{2}m_1^2(\phi-\phi_1)^2+V_1, & \phi<\phi_1,\\ \lambda\left(\phi^2+\frac{1}{2\lambda}\right)^2-\phi^3-\frac{1}{4\lambda}+V_1, & \phi_1\le\phi\le\phi_2,\\ \frac{1}{2}m_2^2(\phi-\phi_2)^2+V_2, & \phi_2<\phi,\end{cases} \tag{1}$$

see Fig. 1. The minima of the fourth-order polynomial are at $\phi_1=0$ and $\phi_2=\frac{3+\sqrt{9-32\lambda}}{8\lambda}$ $(\lambda<\frac{9}{32})$, respectively, at which the potential is differentiable. In the simulation, we will fix $m_1^2=m_2^2=0.2$ and $\lambda=0.2375$.

The initial inhomogeneity of the scalar field ϕ is regarded as

$$\phi|_{t=0}=\phi_0+\Delta\phi\sum_{\vec{x}=x,y,z}\cos\left(\frac{2\pi\vec{x}}{L}\right), \tag{2}$$

similar to that in Refs. [41,42], where $\vec{x}$ is the spatial coordinate, $\Delta\phi$ is the amplitude of initial inhomogeneity, while the length of the simulated cubic region is $L=4$. The initial expansion rates for the dSdS and dSAdS scenarios are $H_{init}=0.7$, 0.6, respectively, corresponding to Hubble radii $H^{-1}=1.43, 1.67<L$; i.e., the initial scale of inhomogeneity is superhorizonal.

In light of the potential in (1), we classify the scenarios simulated as dSdS (both vacua are dS-like) and dSAdS (one is dS-like and the other is AdS-like). We will consider simulations of three cases (for dSdS and dSAdS, respectively),[3] with $\Delta\phi=0.7$ but with different average field values $\phi_0=0.2$, 1.0, 1.7 for dSdS ($\phi_0=0.3$, 1.0, 2.0 for dSAdS), where $\phi_0=0.2, 1.7(0.3, 2.0)$ indicates that the initial distribution of ϕ is biased towards one of the vacua, see Fig. 1. Here, the inhomogeneity considered clearly exceeds the perturbative level. However, during the very early stage of the universe, the initial inhomogeneity might arise from large quantum fluctuations with $\Delta\phi\simeq H$, where $H\sim\mathcal{O}(1)$. In addition, the string landscape conjectures bounds on the scalar field excursion, e.g., in [9,53] $|\Delta\phi|<\mathcal{O}(1)$, is also consistent with our model.

Appendix A shows a brief review on NR based on Baumgarte-Shapiro-Shibata-Nakamura (BSSN) [54,55] and the symbols and conventions in our paper. We set the initial values of BSSN parameters as $\tilde{\gamma}_{ij}=\delta_{ij}$, $\tilde{A}_{ij}=0$, and the initial spatial expansion uniform ($K=$ const. <0) and $\dot{\phi}=0$, which naturally satisfy the momentum constraints. The Hamiltonian constraint is then solved by relaxing χ from the initial value $\chi=1$ with the parabolic equation $\partial_t\chi=\mathcal{H}$. This equation is iterated until it converges (suggesting $\partial_t\chi=\mathcal{H}=0$). The resolution of the simulation is $32\times32\times32$ along the x, y, z axes on the coarsest level with up to three levels of adaptive mesh refinement (AMR) regridding.

III. RESULTS AND ANALYSIS

We will perform the NR simulations with modified GRCHOMBO package to investigate how the field populates the landscape in Fig. 1 in an inhomogeneous universe that is initially expanding.

As a contrast, we first consider a landscape consisting of only dS vacua. We show the evolutions of ϕ at certain regions for dSdS-1,2,3 in Fig. 2. The field initially underwent a rapidly oscillating phase. However, eventually, for dSdS-1 the fields in different spatial regions will separate into different vacua, and the dS bubbles come into being with clear boundaries, while for dSdS-2,3, the overall region will be in a nearly homogeneous dS expansion.

The Hubble rate at a local homogeneous region is

$$H_{\rm local}=\lim_{V\to0}\sqrt{\frac{1}{V}\int\frac{\rho(\phi)}{3}dV}=-\frac{K}{3}, \tag{3}$$

In Fig. 3, for dSdS-1, the local Hubble rate will be $H_{\rm local}=(\frac{V(\phi_{1,2})}{3})^{1/2}$, i.e., at different vacua ϕ_1 and ϕ_2, respectively, and for dSdS-2,3, $H_{\rm local}$ will be identical eventually at all region, i.e., a homogeneous dS expansion. The result is consistent with Fig. 2.

In our simulation results for dSdS-1, eventually the dS bubbles will emerge in a high-energy dS background. It is well known that if the radius of the bubble is larger than the Hubble radius of the background, $r\gtrsim H^{-1}$, then the bubble

[2]This helps to ease the computational cost of relaxing the initial condition.

[3]The result is labeled by the scenario it belongs to (dSdS or dSAdS) followed by the different case numbers, e.g., dSdS-1.

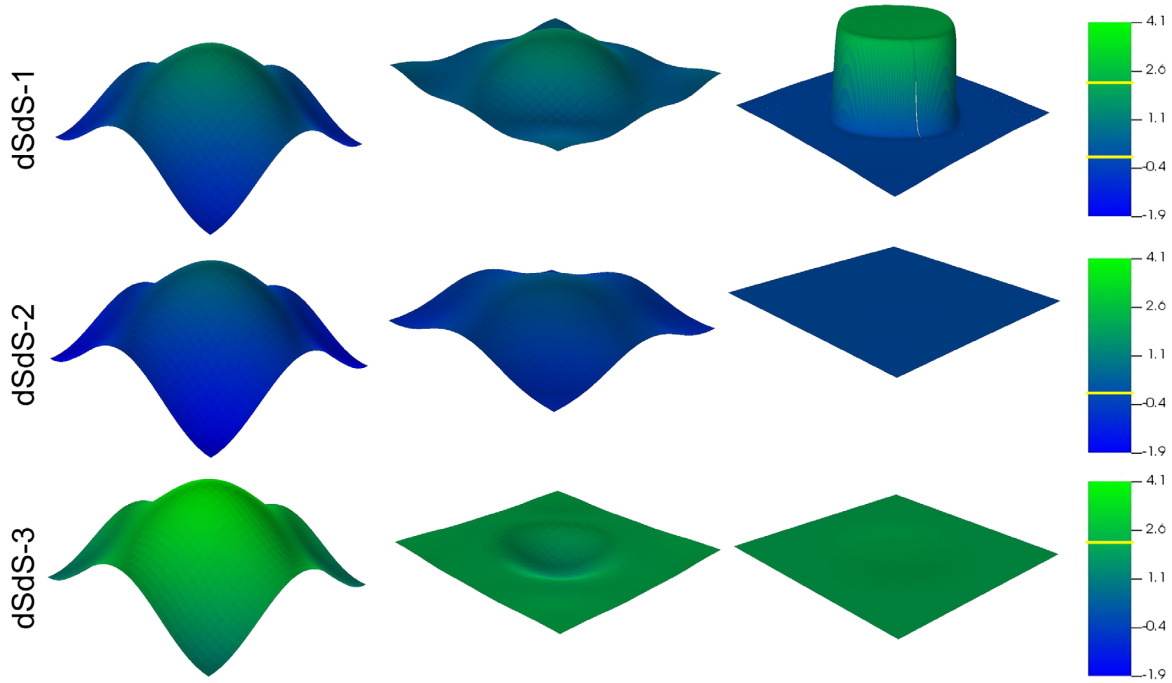

FIG. 2. Results of ϕ at $x-y$ slices at different time steps (proceeding from left to right) for dSdS-1,2,3. The color bar and the elevation height show the value of ϕ. The yellow line on the color bar marks the converged values of ϕ.

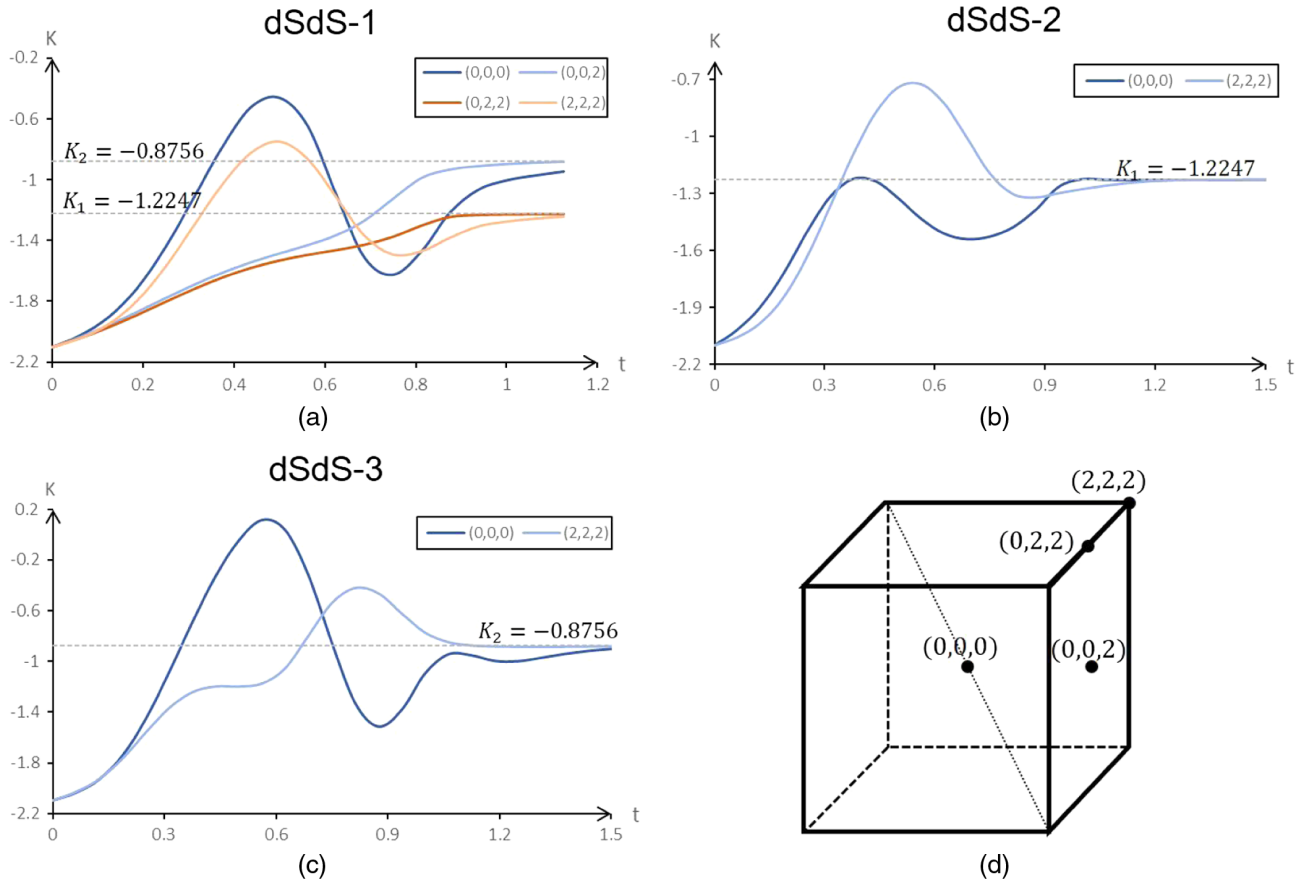

FIG. 3. The evolution of K for dSdS-1,2,3. K_1 and K_2 correspond to the local Hubble rate at ϕ_1 and ϕ_2, respectively [noting both $V(\phi_1), V(\phi_2) > 0$ for dSdS in Fig. 1]. Panel (d) shows the labeling of the positions in (a)–(c). These positions are at the bulk (center) of the vacua or where these regions intersect the simulation boundary, and best capture the physics of corresponding vacua.

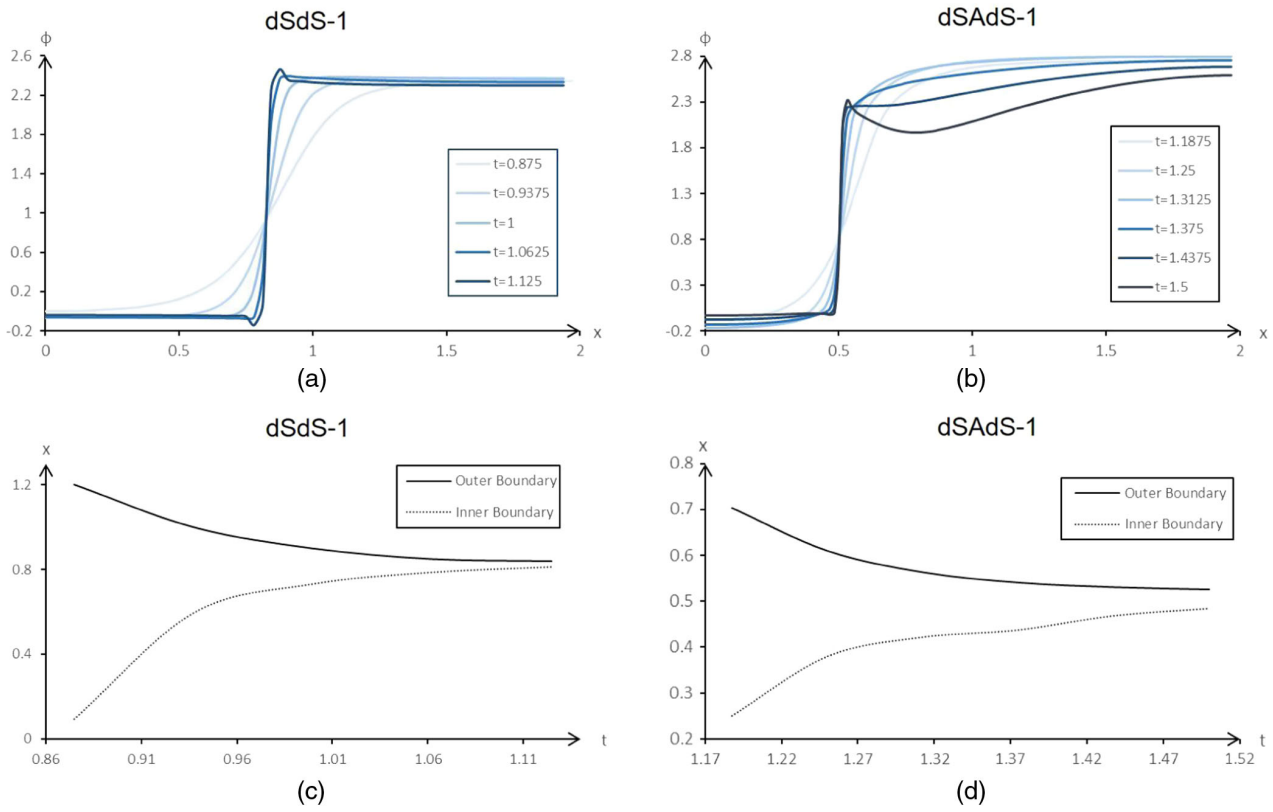

FIG. 4. Upper row: the value of ϕ along the x axis, showing the different vacua regions with $\phi = 2.2$ and $\phi = 0$ separated by a bubble wall. The darker lines show the field configurations for later time. Second row: positions of the inner and outer boundaries of the bubble wall. It is clear that the width of the bubble wall in comoving coordinates shrinks with time, which indicates that the position of the bubble wall freezes.

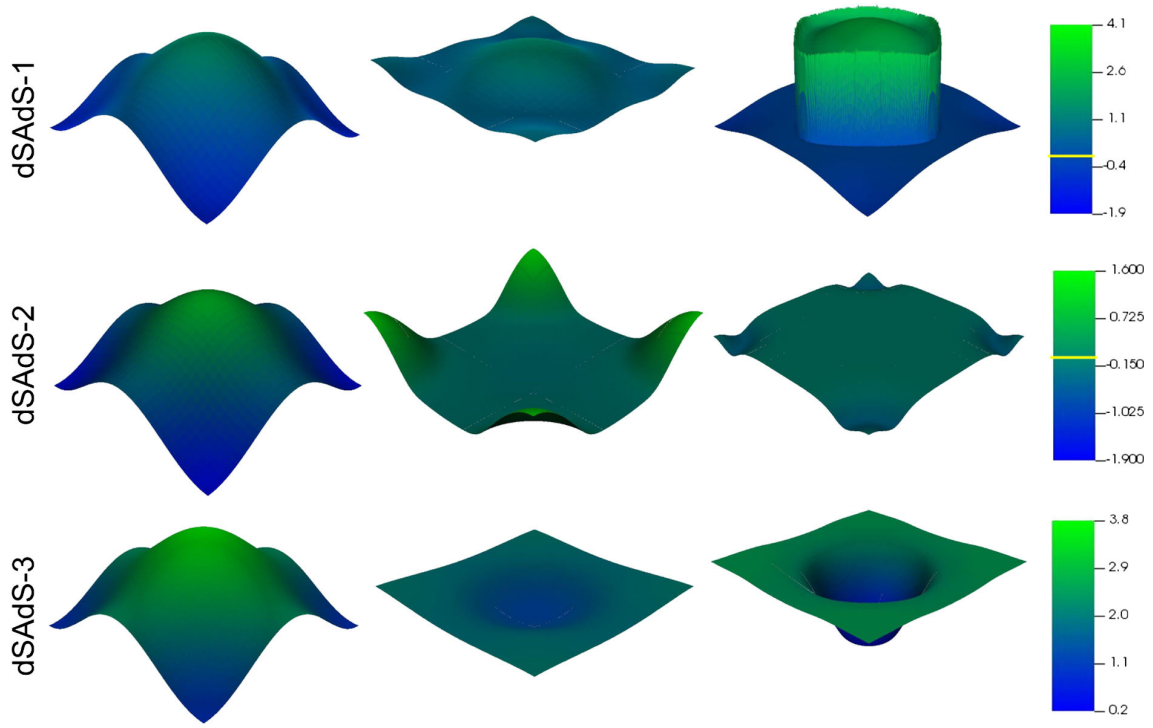

FIG. 5. Results of ϕ at $x - y$ slices at different time steps (proceeding from left to right) for dSAdS-1,2,3. The color bar and the elevation height show the value of ϕ. The yellow line on the color bar marks the converged values of ϕ.

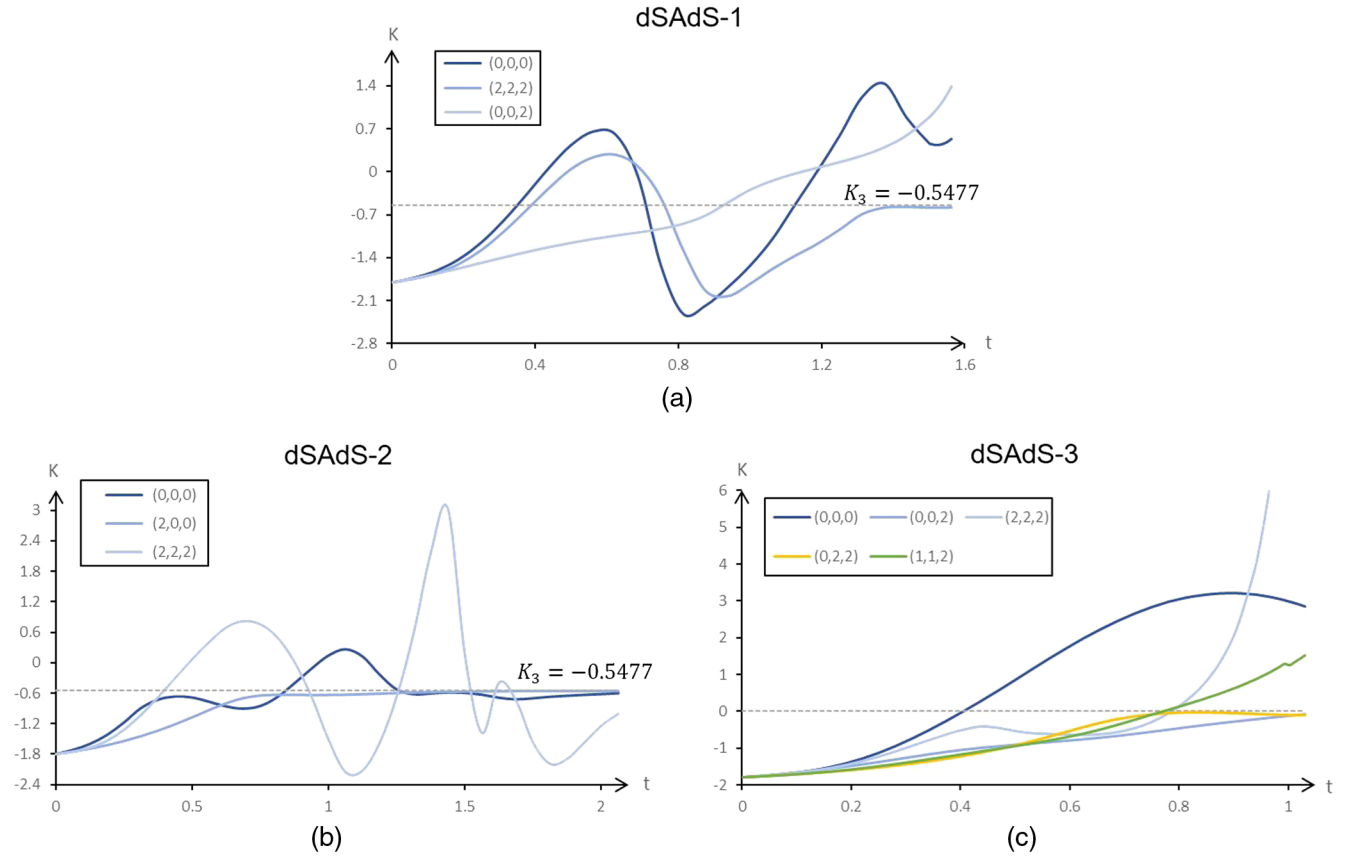

FIG. 6. The evolution of K for dSAdS-1,2,3. K_3 corresponds to the local Hubble rate at ϕ_1 [noting that $V(\phi_1) > 0$ and $V(\phi_2) < 0$ for dSAdS in Fig. 1]. The positions are labeled in accordance with Fig. 3(d).

wall will expand with the background. In Fig. 4, we see that the position of the bubble wall is frozen, suggesting that the dS bubble is in fact expanding with the background. However, the condition $r > 1/H$ is not strictly satisfied in our simulation, the Hubble length H^{-1} of background in dSdS-1 is 2.45, which is comparable but not less than the radius $r \simeq 1$ of bubble.

It is more interesting to investigate the dSAdS landscape in Fig. 1. We show the evolutions of ϕ at different regions for dSAdS-1,2,3 in Fig. 5. Results show that dSAdS behaved similarly to dSdS only at the initial stage of the evolution.

It is significant to check the local expansion rate. In Fig. 6,[4] for dSAdS-1, some regions eventually converged to $H_{\text{local}} = \text{const.} > 0$ (the dS expansion), while other regions have $H_{\text{local}} < 0$. In Fig. 7, these contracting AdS regions will always collapse. Reference [56] investigated a homogeneous case with $V_{\text{min}} < 0$ and showed the diverging property of H once it crosses to the negative side, which indicates the final fate of the AdS bubbles in our simulation. For dSAdS-2, after the initial oscillation, the overall region will have a nearly homogeneous dS expansion, except for a few smaller AdS bubbles, see Fig. 7. Thus our results show that the expanding dS regions may be present eventually, even if the AdS vacua exist. For dSAdS-3, the story is different. Due to the rapid collapse of the AdS spacetime, the numerical code is unable to evolve the system after the collapsing regions run into "singularities" somewhere. In Fig. 7, we see that some regions with $K < 0$ are left at the end of the simulation. However, these regions cannot evolve to a stable dS spacetime, because the profile of ϕ has crossed the potential barrier and fallen in the range of the AdS minima, see the third row of Fig. 5. The corresponding AdS vacua will eventually stop the expansion of these regions and convert them into collapsing spacetime. We thus conclude that the overall region will eventually be AdS-like, resulting in an inhomogeneous collapse.

In our simulation result for dSAdS-1, see Fig. 4, eventually the position of the bubble wall is frozen, suggesting that the wall of AdS bubble is expanding with background, so such AdS bubbles correspond to the separated universes, but the spacetime inside AdS bubbles is contracting (confirming the argument of Ref. [57]). The radius of AdS bubbles is approximately $r < 1/H \simeq 5.48$. Again, as in dSdS-1, the condition $r > 1/H$ is not satisfied. The contracting AdS bubble might be relevant to our universe [12,14,58,59], if a nonsingular bounce happened, which might explain the large-scale CMB power deficit

[4]In our simulation, the calculations will stop whenever a single point in space diverged.

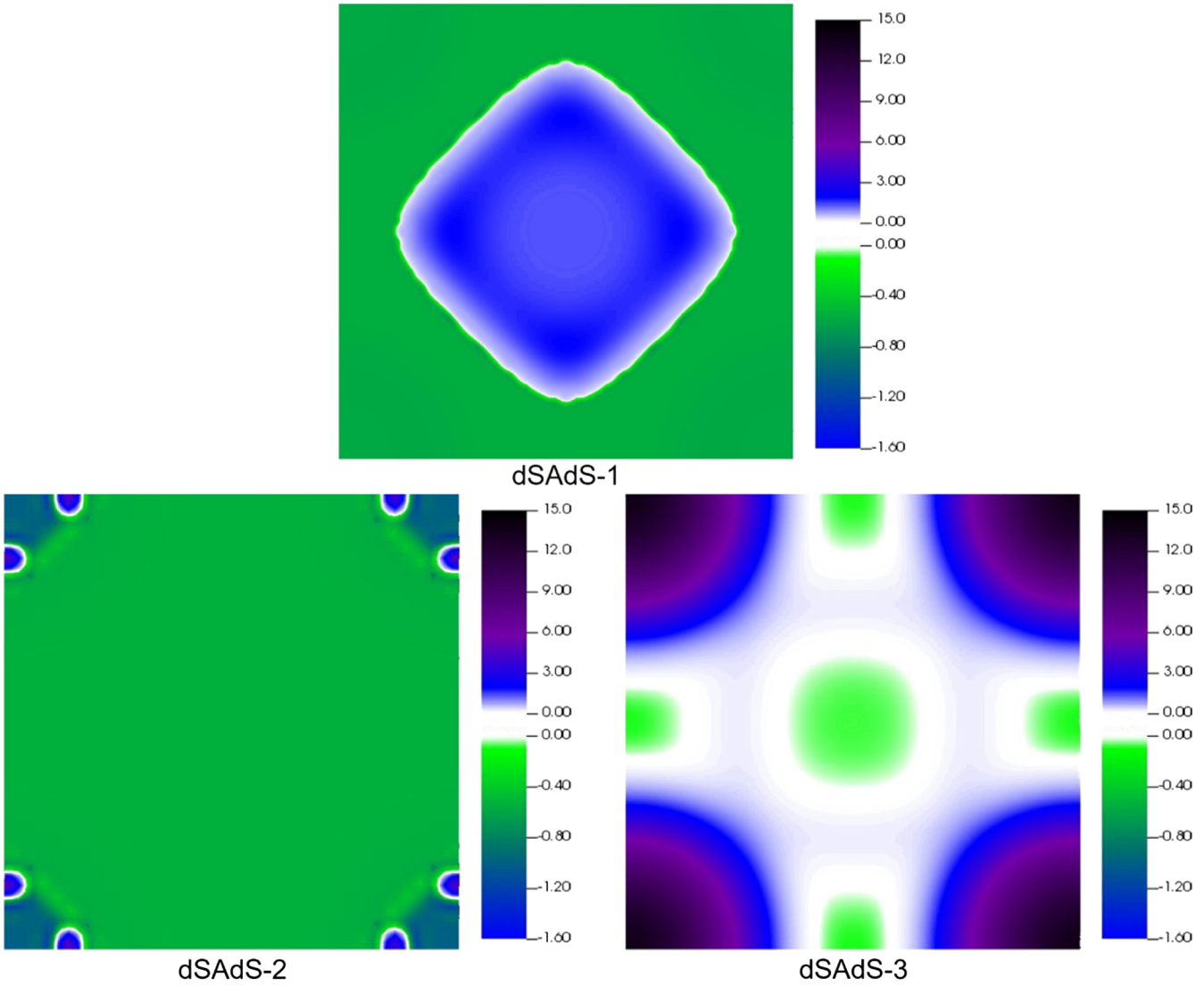

FIG. 7. The values of K for dSAdS-1,2,3 at final time steps. There are two sets of color bars: the upper color bar shows the value of K for $K > 0$ (the contracting region), while the lower color bar shows that for $K < 0$ (the expanding region), the two regions are separated by walls where $K = 0$ is colored in white.

[60–62]. While in dSAdS-2, the AdS bubbles have its radius $r \ll 1/H$, which (to observers outside the bubbles) will then collapse into black holes,[5] see also [15,63].

IV. CONCLUSIONS

It is usually speculated that the primordial universe is highly inhomogeneous, i.e., the scalar field or spacetime metric has large inhomogeneities. How the landscape is populated in an inhomogeneous universe is still a significant question.

In an inhomogeneous universe that is initially expanding, we perform the $(3+1)$D numerical relativity simulations for the evolution of a scalar field in the simplified landscape in Fig. 1, and investigated how the field populates such a landscape. The simulation results showed that, eventually, either the overall region is in a nearly homogeneous dS expansion (for dSAdS, however, a few smaller regions corresponding to AdS bubbles collapsed into black holes), or the whole region is inhomogeneously collapsing, or the field in different spatial region separates into different vacua, so that expanding dS and AdS bubbles (the bubble wall is expanding but the spacetime inside AdS bubbles is contracting) come into being with clear boundaries.

It is noted that the initial high inhomogeneities seem to amplify the probability that different regions of the universe arrive at different vacua. Also, the bubble wall expand with the background seems to not require that the bubble radius must be strictly larger than the Hubble radius. Though we perform the simulation in a simplified landscape, our results have captured relevant physics.

[5]It has been argued in Ref. [42] that the large inhomogeneities of the scalar field may create black holes. However, our case is different, the black holes result from the collapse of AdS bubbles.

The theory of inflation as a paradigm of the early universe indicates the existence of a dS or quasi-dS phase of the universe. Studies on the string landscape had attempted to answer the questions of whether a dS vacua is permitted in string theory and, if so, how can dS vacua be constructed. On the other hand, the initial conditions of the universe is not necessarily (in fact, unlikely) homogeneous. Here, we discuss the questions of how in a highly inhomogeneous universe (where the dS vacua is not yet populated) a patch of spacetime evolves into the dS vacua, if they exist. We showed that the "islands" of dS spacetime can naturally emerge depending on the initial conditions of the field configuration. Thus we actually suggested the possibility for the appearance and existence of local dS spacetime that corresponds to our universe.

An interesting issue that follows is what signals would we "see" if our universe indeed went through such an inhomogeneous evolution before or during inflation?

ACKNOWLEDGMENTS

P. X. L. would like to thank Gen Ye, Hao-Hao Li, Hao-Yang Liu for helpful discussions. We also acknowledge the use of the package GRCHOMBO and VISIT. This work is supported by NSFC, Grants No. 12075246 and No. 11690021, and also the UCAS Undergraduate Innovative Practice Project.

APPENDIX A: A BRIEF REVIEW ON NR AND BSSN FORMALISM

In the context of $3+1$ decomposition of NR, the metric is

$$g_{00} = -\alpha^2 + \beta_i\beta^i, \qquad g_{0i} = \beta_i, \qquad g_{ij} = \gamma_{ij}, \tag{A1}$$

where α is the lapse parameter, β^i the shift vector and γ_{ij} the spatial metric. In order to formulate the evolution of spacetime and the "matter" inside as a well-posed Cauchy problem, the system of partial differential equations should be explicitly written in a hyperbolic form. According to BSSN [54,55], the evolution equations are

$$\partial_t\chi = \frac{2}{3}\alpha\chi K - \frac{2}{3}\chi\partial_k\beta^k + \beta^k\partial_t\chi, \tag{A2}$$

$$\partial_t\tilde{\gamma}_{ij} = -2\alpha\tilde{A}_{ij} + \tilde{\gamma}_{ik}\partial_j\beta^k + \tilde{\gamma}_{jk}\partial_i\beta^k - \frac{2}{3}\tilde{\gamma}_{ij}\partial_k\beta^k + \beta^k\partial_k\tilde{\gamma}_{ij}, \tag{A3}$$

$$\partial_t K = -\tilde{\gamma}^{ij}D_iD_j\alpha + \alpha\left(\tilde{A}_{ij}\tilde{A}^{ij} + \frac{1}{3}K^2\right) + \beta^i\partial_i K + 4\pi G\alpha(\rho + S), \tag{A4}$$

$$\partial_t\tilde{A}_{ij} = \chi[-D_iD_j\alpha + \alpha(R_{ij} - 8\pi\alpha S_{ij})]^{TF} + \alpha(K\tilde{A}_{ij} - 2\tilde{A}_{il}\tilde{A}) + \tilde{A}_{ik}\partial_j\beta^k + \tilde{A}_{jk}\partial_i\beta^k - \frac{2}{3}\tilde{A}_{ij}\partial_k\beta^k + \beta^k\partial_k\tilde{A}_{ij}, \tag{A5}$$

$$\begin{aligned}\partial_t\tilde{\Gamma}^i = {} & -2\tilde{A}^{ij}\partial_j\alpha + 2\alpha\left(\tilde{\Gamma}^i_{jk}\tilde{A}^{jk} - \frac{2}{3}\tilde{\gamma}^{ij}\partial_j K - \frac{3}{2\chi}\tilde{A}^{ij}\partial_j\chi\right) + \beta^k\partial_k\tilde{\Gamma}^i + \tilde{\gamma}^{jk}\partial_j\partial_k\beta^i \\ & + \frac{1}{3}\tilde{\gamma}^{ij}\partial_j\partial_k\beta^k + \frac{2}{3}\tilde{\Gamma}^i\partial_k\beta^k - \tilde{\Gamma}^k\partial_k\beta^i - 16\pi G\alpha\tilde{\gamma}^{ij}S_j,\end{aligned} \tag{A6}$$

where the tilde represents the conformal quantities $\tilde{\gamma}_{ij} = \chi\gamma_{ij}$, $\tilde{\Gamma}^i \equiv \tilde{\gamma}^{jk}\tilde{\Gamma}^i_{jk}$ and K is the extrinsic curvature. The Hamiltonian and momentum constraints are

$$\mathcal{H} = \tilde{D}^2\chi - \frac{5}{4\chi}\tilde{\gamma}^{ij}\tilde{D}_i\chi\tilde{D}_j\chi + \frac{\chi\tilde{R}}{2} + \frac{K^2}{3} - \frac{1}{2}\tilde{A}^{ij}\tilde{A}_{ij} - 8\pi G\rho = 0, \tag{A7}$$

$$\mathcal{M}^i = \tilde{D}_j\tilde{A}^{ij} - \frac{3}{2\chi}\tilde{A}^{ij}\tilde{D}_j\chi - \frac{2}{3}\tilde{\gamma}^{ij}\tilde{D}_j K - 8\pi G\Pi\tilde{\gamma}^{ij}\partial_j\phi = 0. \tag{A8}$$

The Klein-Gordon equation of canonical scalar field ϕ is $\Box\phi = -V'$. According to BSSN, it is rewritten as [52] [with the momentum conjugate $\Pi = \frac{1}{\alpha}(\partial_t\phi - \beta^i\partial_i\phi)$]

$$\partial_t\Pi = \alpha(K\Pi - \Gamma^k\partial_k\phi - V') + \alpha\partial_i\partial^i\phi + \partial_i\phi\partial^i\alpha + \beta^i\partial_i\Pi. \tag{A9}$$

The gauge conditions in our simulations are the 1+log slicing and the Eulerian gauge,

$$\partial_t\alpha = -2\alpha K + \beta^i\partial_i\alpha, \qquad \beta^i = 0, \tag{A10}$$

see, e.g., [64–67] for details.

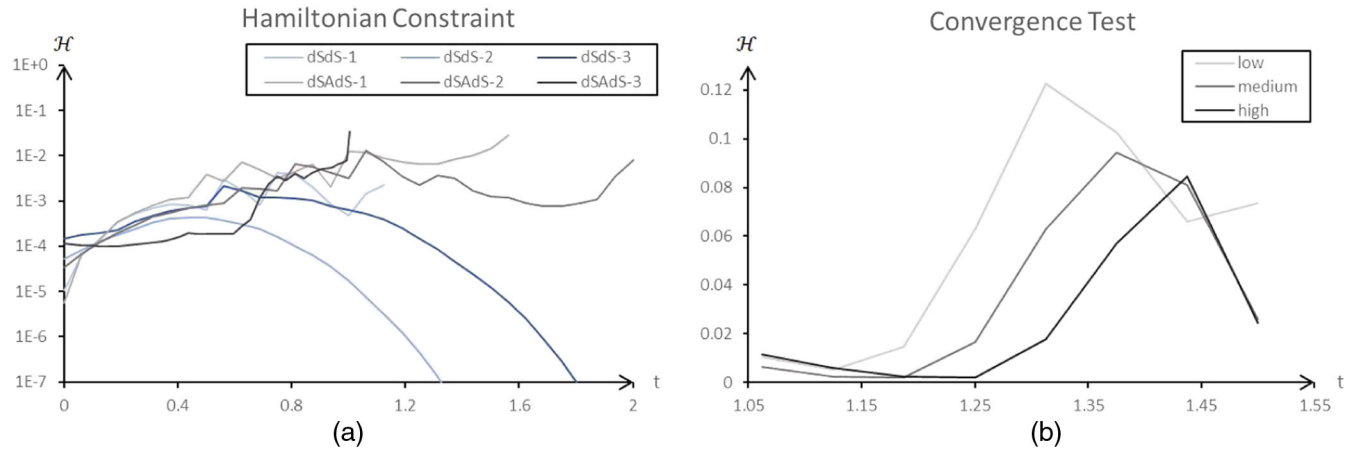

FIG. 8. (a) The box-averaged L_2 norm of the Hamiltonian constraint $\mathcal{H}$. Due to the fact that the Hamiltonian of different points can cross $H = 0$, a fraction Hamiltonian violation cannot be globally defined. Thus, with the data yielding the average $H \sim O(1)$, we instead keep the absolute constraint violation under 10^{-2}. (b) A convergence test with different grid resolutions. The presented results shows the Hamiltonian violation of case dSAdS-1 when the bubble wall formed. Higher resolution yields higher precision at the start of the bubble wall formation, afterwards, the results under medium and high resolutions start to converge.

APPENDIX B: ON HAMILTONIAN CONSTRAINT AND CONVERGENCE TEST

Figure 8 shows the Hamiltonian constraint violation throughout the numerical simulation for all simulated cases and a convergence test we performed on dSAdS-1.

[1] A. H. Guth, Phys. Rev. D **23**, 347 (1981).
[2] A. D. Linde, Phys. Lett. **108B**, 389 (1982).
[3] A. Albrecht and P. J. Steinhardt, Phys. Rev. Lett. **48**, 1220 (1982).
[4] A. A. Starobinsky, Phys. Lett. B **91B**, 99 (1980).
[5] K. Sato, Mon. Not. R. Astron. Soc. **195**, 467 (1981).
[6] L. Z. Fang, Phys. Lett. B **95B**, 154 (1980).
[7] R. Bousso and J. Polchinski, J. High Energy Phys. 06 (2000) 006.
[8] L. Susskind, arXiv:0302219v1.
[9] H. Ooguri and C. Vafa, Nucl. Phys. **B766**, 21 (2007).
[10] G. Obied, H. Ooguri, L. Spodyneiko, and C. Vafa, arXiv: 1806.08362.
[11] U. H. Danielsson, S. S. Haque, G. Shiu, and T. Van Riet, J. High Energy Phys. 09 (2009) 114.
[12] Y.-S. Piao, Phys. Rev. D **70**, 101302 (2004).
[13] Y.-S. Piao and Y.-Z. Zhang, Nucl. Phys. **B725**, 265 (2005).
[14] J. Garriga, A. Vilenkin, and J. Zhang, J. Cosmol. Astropart. Phys. 11 (2013) 055.
[15] J. J. Blanco-Pillado, H. Deng, and A. Vilenkin, J. Cosmol. Astropart. Phys. 05 (2020) 014.
[16] H.-H. Li, G. Ye, Y. Cai, and Y.-S. Piao, Phys. Rev. D **101**, 063527 (2020).
[17] G. Ye and Y.-S. Piao, Phys. Rev. D **101**, 083507 (2020).
[18] G. Ye and Y.-S. Piao, Phys. Rev. D **102**, 083523 (2020).
[19] S. R. Coleman, Phys. Rev. D **15**, 2929 (1977); **16**, 1248(E) (1977).
[20] S. R. Coleman and F. De Luccia, Phys. Rev. D **21**, 3305 (1980).
[21] S. K. Blau, E. I. Guendelman, and A. H. Guth, Phys. Rev. D **35**, 1747 (1987).
[22] K.-M. Lee and E. J. Weinberg, Phys. Rev. D **36**, 1088 (1987).
[23] A. D. Linde, Nucl. Phys. **B372**, 421 (1992).
[24] R. Easther, J. T. Giblin, Jr., L. Hui, and E. A. Lim, Phys. Rev. D **80**, 123519 (2009).
[25] A. R. Brown and A. Dahlen, Phys. Rev. Lett. **107**, 171301 (2011).
[26] J. Braden, M. C. Johnson, H. V. Peiris, A. Pontzen, and S. Weinfurtner, Phys. Rev. Lett. **123**, 031601 (2019).
[27] J. J. Blanco-Pillado, H. Deng, and A. Vilenkin, J. Cosmol. Astropart. Phys. 12 (2019) 001.
[28] H. Huang and L. H. Ford, arXiv:2005.08355.
[29] S.-J. Wang, Phys. Rev. D **100**, 096019 (2019).
[30] M. Li and Y. Wang, J. Cosmol. Astropart. Phys. 07 (2009) 033.
[31] S. Li, Y. Liu, and Y.-S. Piao, Phys. Rev. D **80**, 123535 (2009).
[32] T. Cai, J. Jiang, and Y. Wang, arXiv:2110.05268.
[33] L. Lehner and F. Pretorius, Annu. Rev. Astron. Astrophys. **52**, 661 (2014).

[34] V. Cardoso, L. Gualtieri, C. Herdeiro, and U. Sperhake, Living Rev. Relativity **18**, 1 (2015).
[35] C. Palenzuela, Front. Astron. Space Sci. **7**, 58 (2020).
[36] J. T. Giblin, J. B. Mertens, and G. D. Starkman, Phys. Rev. Lett. **116**, 251301 (2016).
[37] H. J. Macpherson, P. D. Lasky, and D. J. Price, Phys. Rev. D **95**, 064028 (2017).
[38] H. J. Macpherson, D. J. Price, and P. D. Lasky, Phys. Rev. D **99**, 063522 (2019).
[39] J. T. Giblin and A. J. Tishue, Phys. Rev. D **100**, 063543 (2019).
[40] X.-X. Kou, C. Tian, and S.-Y. Zhou, Classical Quantum Gravity **38**, 045005 (2021).
[41] W. E. East, M. Kleban, A. Linde, and L. Senatore, J. Cosmol. Astropart. Phys. 09 (2016) 010.
[42] K. Clough, E. A. Lim, B. S. DiNunno, W. Fischler, R. Flauger, and S. Paban, J. Cosmol. Astropart. Phys. 09 (2017) 025.
[43] K. Clough, R. Flauger, and E. A. Lim, J. Cosmol. Astropart. Phys. 05 (2018) 065.
[44] J. C. Aurrekoetxea, K. Clough, R. Flauger, and E. A. Lim, J. Cosmol. Astropart. Phys. 05 (2020) 030.
[45] C. Joana and S. Clesse, Phys. Rev. D **103**, 083501 (2021).
[46] M. C. Johnson, H. V. Peiris, and L. Lehner, Phys. Rev. D **85**, 083516 (2012).
[47] C. L. Wainwright, M. C. Johnson, H. V. Peiris, A. Aguirre, L. Lehner, and S. L. Liebling, J. Cosmol. Astropart. Phys. 03 (2014) 030.
[48] C. L. Wainwright, M. C. Johnson, A. Aguirre, and H. V. Peiris, J. Cosmol. Astropart. Phys. 10 (2014) 024.
[49] M. C. Johnson, C. L. Wainwright, A. Aguirre, and H. V. Peiris, J. Cosmol. Astropart. Phys. 07 (2016) 020.
[50] Z. Nazari, M. Cicoli, K. Clough, and F. Muia, J. Cosmol. Astropart. Phys. 05 (2021) 027.
[51] E. de Jong, J. C. Aurrekoetxea, and E. A. Lim, arXiv: 2109.04896.
[52] K. Clough, P. Figueras, H. Finkel, M. Kunesch, E. A. Lim, and S. Tunyasuvunakool, Classical Quantum Gravity **32**, 245011 (2015).
[53] P. Agrawal, G. Obied, P. J. Steinhardt, and C. Vafa, Phys. Lett. B **784**, 271 (2018).
[54] T. W. Baumgarte and S. L. Shapiro, Phys. Rev. D **59**, 024007 (1998).
[55] M. Shibata and T. Nakamura, Phys. Rev. D **52**, 5428 (1995).
[56] G. N. Felder, A. V. Frolov, L. Kofman, and A. D. Linde, Phys. Rev. D **66**, 023507 (2002).
[57] L. F. Abbott and S. R. Coleman, Nucl. Phys. **B259**, 170 (1985).
[58] Y.-S. Piao, Phys. Lett. B **677**, 1 (2009).
[59] M. C. Johnson and J.-L. Lehners, Phys. Rev. D **85**, 103509 (2012).
[60] Y.-S. Piao, B. Feng, and X.-M. Zhang, Phys. Rev. D **69**, 103520 (2004).
[61] Z.-G. Liu, Z.-K. Guo, and Y.-S. Piao, Phys. Rev. D **88**, 063539 (2013).
[62] Y. Cai, Y.-T. Wang, J.-Y. Zhao, and Y.-S. Piao, Phys. Rev. D **97**, 103535 (2018).
[63] J. Garriga, A. Vilenkin, and J. Zhang, J. Cosmol. Astropart. Phys. 02 (2016) 064.
[64] M. Alcubierre, *Introduction to 3+1 Numerical Relativity* (Oxford University Press, New York, 2008), Vol. 140.
[65] T. W. Baumgarte and S. L. Shapiro, *Numerical Relativity: Solving Einstein's Equations on the Computer* (Cambridge University Press, Cambridge, England, 2010).
[66] E. Gourgoulhon, arXiv:gr-qc/0703035.
[67] L. Lehner, Classical Quantum Gravity **18**, R25 (2001).